

Density Functional Theory Study of CL-20/Nitroimidazoles Energetic Cocrystal Compounds in an External Electric Field

xiaosong Xu

Nanjing Tech University

Renfa Zhang

Nanjing Tech University

Wenxin Xia

Nanjing Tech University

Peng Ma (✉ mapeng@njtech.edu.cn)

Nanjing Tech University

Congming Ma

Nanjing Tech University

Yong Pan

Nanjing Tech University

Juncheng Jiang

Nanjing Tech University

Research Article

Keywords: external electric field, density functional theory, energetic cocrystal materials, nitroimidazoles

Posted Date: August 10th, 2021

DOI: <https://doi.org/10.21203/rs.3.rs-768607/v1>

License:   This work is licensed under a Creative Commons Attribution 4.0 International License.

[Read Full License](#)

Abstract

The external electric field has a significant influence on the sensitivity of the energetic cocrystal materials. In order to find out the relationship between the external electric field and sensitivity of energetic cocrystal compounds 2,4,6,8,10,12-hexanitro-2,4,6,8,10,12-hexaazaisowurtzitane/1,4-dinitroimidazole (CL-20/1,4-DNI), 2,4,6,8,10,12-hexanitro-2,4,6,8,10,12-hexaazaisowurtzitane/1-methyl-2,4-dinitro-1H-imidazole (CL-20/2,4-MDNI) and 2,4,6,8,10,12-hexanitro-2,4,6,8,10,12-hexaazaisowurtzitane/1-methyl-4,5-dinitro-1H-imidazole (CL-20/4,5-MDNI). In this work, density functional theory (DFT) at B3LYP-D3/6-311+G(d,p) and M062X-D3/ma-def2 TZVPP levels was employed to calculate the bond dissociation energies (BDEs) of selected $N-NO_2$ trigger bonds, frontier molecular orbitals, electrostatic potentials (ESPs) and nitro group charges (QNO2) under different external electric field. The results show that as the positive electric field intensity increases, the highest occupied molecular orbital (HOMO) and the lowest unoccupied molecular orbital (LUMO) energy gap and BDEs become smaller, and the local positive ESPs becomes larger, so that the energetic cocrystals tends to have higher sensitivity. In addition, the linear fitting results show that the trigger bond length and nitro group charge changes are closely related to the external electric field strength.

1 Introduction

In recent years, energetic cocrystal materials have attracted much attention due to their excellent detonation properties [1–4]. Studying the effect of external electric field on energetic cocrystal molecules will help us understand the characteristics of this material and help us purposefully synthesize high-performance new explosives [5–6].

Usually, energetic materials have some energetic groups, which makes such materials release a large amount of energy under certain conditions, making them have great potential value in many fields such as military and propellant [7]. 2,4,6,8,10,12-Hexanitro-2,4,6,8,10,12-hexaazaisowurtzitane (CL-20) is a fourth-generation, caged nitroimine explosive. Also, it is the most powerful non-nuclear elementary explosive that can be used in practical applications [8]. However, the high mechanical sensitivity of CL-20 significantly impairs its safety and severely limit the application of CL-20. Co-crystallization technology is often used in the pharmaceutical industry to modify drug molecules to achieve specific properties. In recent years, this technology has been introduced by researchers to reduce the sensitivity of explosives, and co-crystallization technology is receiving increasing attention in the field of synthesizing new energetic materials [9–14]. By dissolving two explosives in the same solvent, according to the characteristics of the two explosive molecules, different methods are used to make the cocrystal precipitate in the solution, so that the two explosive molecules are combined into the same crystal lattice through weak intermolecular interactions. This kind of supramolecular thus has a specific crystal structure and properties [15–17]. Using a material with lower mechanical sensitivity as a ligand to form a cocrystal with CL-20 is one of the effective methods to reduce the high mechanical sensitivity of CL-20. Recently, CL-20 has been co-crystallized with nitroimidazoles [1,4-dinitroimidazole (1,4-DNI), 1-methyl-2,4-dinitro-1H-imidazole (2,4-MDNI), and 1-methyl-4,5-dinitro-1H-imidazole (4,5-MDNI)]. Due to the existence

of the nitro groups, the nitroimidazoles contains relatively large energy. After forming a cocrystal with CL-20, it can significantly improve the detonation performance of the cocrystal. In 2018 Yang et al. [18] prepared CL-20/2,4-MDNI and CL-20/4,5-MDNI cocrystal, both cocrystals have high density, high detonation performance, low sensitivity and excellent thermal stability. In 2019, Tan et al. [19] prepared CL-20/1,4-DNI cocrystal, which has excellent detonation performance and can be used as a substitute for 1,3,5,7-tetranitro-1,3,5,7-tetraazacyclooctane (HMX) in the future. However, the mechanical sensitivity and other properties of these three cocrystal molecules (CL-20/1,4-DNI, CL-20/2,4-MDNI and CL-20/4,5-MDNI) under electric field is rarely studied. Therefore, this work aims to find the relationship between the external electric field and the mechanical sensitivity of the three cocrystal molecules by quantum chemistry theory.

Li et al [20] used theoretical calculations to study the changes in the structure and electrons of lead azide crystals induced by an electric field. Ren et al [21–22] conducted a theoretical study on the possible trigger linkage theory prediction of CH_3NO_2 and NH_2NO_2 in an external electric field and a theoretical study on the hydrogen transfer kinetics of the $\text{NH}_2\text{NO}_2 \cdots \text{H}_2\text{O}$ complex in an external electric field. Sun et al. [23] has studied the theoretical prediction of CL-20's trigger linkage, cage strain and explosive sensitivity under the external electric field. Wu et al [24] studied the external electric field induced conformational changes as a buffer to increase the stability of the CL-20/HMX cocrystal and its pure components. In recent years, since the trigger bond of nitroimine explosives is usually $N\text{-NO}_2$, the role of electron and nitro oxygen transfer in the trigger reaction of energetic materials has attracted more and more attention [25]. Therefore, to reveal the essence of the influence of the external electric field on the sensitivity of the energetic cocrystal compounds, in this work, we used the theoretical calculation method based on DFT to study three kinds of cocrystal (CL-20/1,4-DNI, CL-20/2,4-MDNI, CL-20/4,5-MDNI), and explore the effects of different electric field on the performance of the three cocrystals. This theoretical study will help us better understand the sensitivity change and the explosion mechanism of energetic cocrystal compounds under the external electric field.

2 Computational Details

In this work, all the calculations were performed with the Gaussian 16 software package [26]. The B3LYP-D3/6-311 + G(d,p) method was used to fully optimize the molecular structures of the three cocrystals under the external electric field and no external electric field. The stability of the cocrystal structures is judged by the criteria of "no imaginary frequency" and "reaching four convergence conditions". Subsequently, the M062X-D3/ma-def2 TZVPP method was selected to calculate the single-point energy of the three cocrystal molecules.

After Laplace bond-level analysis, three kinds of cocrystal trigger bonds are obtained, all of which are $N\text{-NO}_2$, as shown in the red box in Fig. 1. Existing research shows that the external electric field perpendicular to the direction of the trigger bond has no obvious effect on the strength of the trigger bond [27], and only the external electric field parallel to the direction of the trigger bond can have a significant effect on the strength of the trigger bond. In order to explore the influence of the applied electric field on

the trigger bond of the cocrystal explosive, the direction of the positive applied electric field is defined as $N \rightarrow NO_2$, and the direction of the negative applied electric field is defined as $NO_2 \rightarrow N$. The field strengths of the applied electric field are as follow: 0.000, ± 0.005 , ± 0.0075 and ± 0.010 a.u., respectively. Figure 1 shows the stable cocrystal molecular structures obtained after optimization on the B3LYP-D3/6-311 + G(d,p) level when no electric field is applied.

3 Results And Discussion

3.1 Change in the Trigger Bond

Research results show that as the cocrystal trigger bond becomes longer, the BDEs and the strength of the trigger bond decreases and the cocrystal sensitivity increases [28]. The changes of the three cocrystal sensitivity were explored by studying the variation of the $N-NO_2$ trigger bond length under the external electric field. The variation of trigger bond length is shown in Table 1. Under the positive electric field, as the electric field intensity increases, the trigger bonds of the three cocrystal molecules all become longer, indicating that their sensitivity becomes higher. Under the negative electric field, the situation is reversed.

To clearly show the influence of the external electric field on the trigger bond length, a linear fit was performed on the change of the trigger bond length in the external electric field, the fitting results of the ΔR_{N-NO_2} of the three cocrystals under the electric field are shown in Fig. 2. The linear correlation coefficients R^2 are 0.976 (CL-20/1,4-DNI), 0.958 (CL-20/2,4-MDNI), 0.977 (CL-20/4,5-MDNI), respectively, which shows that ΔR_{N-NO_2} has a good correlation with electric field intensity.

Table.1 The trigger bond length of energetic cocrystal molecules under different electric fields.

	External electric field/a.u.	$R_{N-NO_2}/\text{\AA}$	$\Delta R_{N-NO_2}/\text{\AA}$
CL-20/1,4-DNI	0.010	1.4780	0.0351
	0.0075	1.4660	0.0231
	0.005	1.4554	0.0125
	0.000	1.4429	0.0000
	-0.005	1.4296	-0.0133
	-0.0075	1.4071	-0.0358
	-0.010	1.4009	-0.0420
CL-20/2,4-MDNI	0.010	1.4206	0.0120
	0.0075	1.4157	0.0071
	0.005	1.4102	0.0016
	0.000	1.4086	0.0000
	-0.005	1.3987	-0.0099
	-0.0075	1.3912	-0.0174
	-0.010	1.3844	-0.0242
CL-20/4,5-MDNI	0.010	1.5094	0.0651
	0.0075	1.4973	0.0530
	0.005	1.4862	0.0419
	0.000	1.4443	0.0000
	-0.005	1.4281	-0.0162
	-0.0075	1.4153	-0.0290
	-0.010	1.4118	-0.0325

To further explore the influence of the external electric field on the cocrystal sensitivity, the bond dissociation energy (EBDE) and interaction energy (Eint) of the three cocrystal molecules were calculated. The calculation results are shown in Table 2. It can be seen from Table 2 that under the external electric field, the variation trend of the Eint of the three cocrystal molecules is different, indicating that there are certain limitations in judging the cocrystal sensitivity from the Eint. As the positive electric field intensity increases, the EBDE of trigger bonds is smaller and the cocrystal sensitivity is higher. When the negative electric field intensity increases, the EBDE of trigger bonds increases and the cocrystal sensitivity

decreases. Under the external electric field, the order of the EBDE of the three cocrystals is as follows: CL-20/2,4-MDNI (48.88 kcal·mol⁻¹) > CL-20/1,4-DNI (47.37 kcal·mol⁻¹) > CL-20/4,5-MDNI (44.37 kcal·mol⁻¹). Therefore, the order of the sensitivity of the three cocrystals is: CL-20/4,5-MDNI > CL-20/1,4-DNI > CL-20/2,4-MDNI. The order of sensitivity obtained by calculating the EBDE is consistent with the order of sensitivity obtained by ESP analysis.

Table.2 Bond dissociation energy and interaction energy of energetic cocrystal materials under different electric fields.

	External electric field/a.u.	$E_{int}/(\text{kcal}\cdot\text{mol}^{-1})$	$E_{BDE}/(\text{kcal}\cdot\text{mol}^{-1})$
CL-20/1,4-DNI	0.010	-6.30	37.59
	0.0075	-5.62	40.41
	0.005	-6.92	44.40
	0.000	-6.65	46.57
	-0.005	-7.86	49.99
	-0.0075	-10.87	55.10
	-0.010	-10.40	57.55
CL-20/2,4-MDNI	0.010	-8.37	42.59
	0.0075	-9.07	44.76
	0.005	-10.41	45.28
	0.000	-12.80	47.52
	-0.005	-18.78	49.06
	-0.0075	-20.66	55.68
	-0.010	-22.37	57.30
CL-20/4,5-MDNI	0.010	-10.77	40.14
	0.0075	-10.83	41.46
	0.005	-11.82	43.85
	0.000	-14.18	45.19
	-0.005	-12.84	45.68
	-0.0075	-11.72	46.10
	-0.010	-10.35	48.23

3.2 Frontier Molecular Orbitals

The highest occupied molecular orbital (HOMO) and the lowest occupied molecular orbital (LUMO) are two important aspects of the frontier molecular orbitals (FMOs) [29]. In addition to the orbitals, the energy gap between HOMO and LUMO also has important physical significance. It can determine the dynamic stability, chemical reactivity and optical polarizability of high-energy materials. The distribution of the HOMO and LUMO of CL-20/1,4-DNI, CL-20/2,4-MDNI and CL-20/4,5-MDNI along with their energy gap is presented in Fig.3. It can be seen from Fig 3(a) that in most cases, the LUMO of CL-20/1,4-DNI is mainly distributed around the nitro group of 1,4-DNI, except when the electric field is -0.005 a.u., at this time LUMO is distributed around the nitro group of CL-20. HOMO is mainly distributed on the imidazole ring of 1,4-DNI, except when the electric field is +0.01 a.u., at this time HOMO is distributed around the nitro group of CL-20. For CL-20/2,4-MDNI, LUMO is mainly distributed on the nitro group of 2,4-MDNI in most cases. In the positive electric field, HOMO is mainly distributed on the nitro group of CL-20. In the negative electric field and no electric field, HOMO is mainly distributed on the imidazole ring of 2,4-MDNI. For CL-20/4,5-MDNI, in any electric field, LUMO is mainly distributed on the nitro group of 4,5-MDNI and HOMO is mainly distributed on the imidazole ring of 4,5-MDNI. Previous studies have shown that FMOs has a greater impact on chemical reactivity [30]. The larger the energy gap of HOMO and LUMO, the lower the chemical activity and the more stable the molecule. The average energy gaps of the three cocrystals are 4.366 eV (CL-20/1,4-DNI), 3.84 eV (CL-20/2,4-MDNI), 4.362 eV (CL-20/4,5-MDNI), respectively. Therefore, among the three cocrystals, CL-20/2,4-MDNI has the highest sensitivity.

3.3 Electrostatic Potential

ESP is an important physical characteristic for studying the interaction, charge distribution and chemical reactivity on the surface of molecules [31]. This section uses the Multiwfn [32] software to calculate the surface ESP of three cocrystal molecules under the external electric field, as shown in Fig.4~6. The maximum surface ESP, minimum surface ESP and the extreme values of the local positive ESP of the trigger bond are shown in Table 3.

It can be seen from Table 3 that with the increase of the electric field intensity, the maximum and minimum surface ESP of CL-20/2,4-MDNI and CL-20/4,5-MDNI both increases. The change of surface ESP value is consistent with the figure of cocrystal surface ESP, which shows that the electric field has a significant effect on the movement of the charge [33]. Under the external electric field, combining Fig.4~6 and Fig.7, part of the blue area of CL-20/1,4-DNI and CL-20/4,5-MDNI turns red, indicating that part of the negative ESP has changed to positive ESP. Under the positive electric field, as the electric field intensity increases, the negative ESP on the molecular surface of CL-20/2,4-MDNI also transforms into the positive ESP. Under the negative electric field, the situation is reversed. All the above changes indicate that the change of cocrystal charge distribution brings about the change of cocrystal sensitivity.

Politzer and Murray [34] point out that the smaller the local positive ESP ($V_{s,max}$) of the trigger bond, the lower the sensitivity of the energetic material and the more stable the energetic material. To explore the change of the trigger bond under the external electric field, the local positive ESP of the trigger bonds of the cocrystal molecules are shown in Table 3. The obtained results show that as the intensity of the positive electric field gradually increases, $V_{s,max}$ also increases, so the cocrystal sensitivity gradually increases. Therefore, the order of the sensitivity of the three cocrystals is: CL-20/4,5-MDNI > CL-20/1,4-DNI > CL-20/2,4-MDNI.

Table.3 The maximum/minimum surface electrostatic potential and trigger bond local positive electrostatic potential extreme value of cocrystals at different electric field.

	External electric field/a.u.	$V_{\max}/(\text{kcal}\cdot\text{mol}^{-1})$	$V_{\min}/(\text{kcal}\cdot\text{mol}^{-1})$	$V_{s\max}/(\text{kcal}\cdot\text{mol}^{-1})$
CL-20/1,4-DNI	0.010	77.14	-51.68	52.42
	0.0075	71.73	-48.11	50.72
	0.005	67.20	-37.25	49.22
	0.000	71.33	-36.58	47.97
	-0.005	72.40	-32.63	33.38
	-0.0075	70.51	-35.73	31.77
	-0.010	72.27	-40.80	26.09
CL-20/2,4-MDNI	0.010	74.92	-50.59	47.58
	0.0075	69.85	-44.68	39.93
	0.005	64.43	-39.69	35.20
	0.000	52.26	-31.99	32.13
	-0.005	66.79	-32.95	29.78
	-0.0075	73.06	-38.72	26.28
	-0.010	79.47	-44.69	19.60
CL-20/4,5-MDNI	0.010	72.08	-38.51	57.48
	0.0075	67.27	-36.21	50.47
	0.005	61.40	-31.77	48.63
	0.000	52.15	-25.54	47.26
	-0.005	65.76	-31.13	38.12
	-0.0075	69.61	-36.02	34.28
	-0.010	74.05	-40.87	30.62

3.4 Nitro Group Charge

Existing studies [35] have shown that the charge of the nitro group of an energetic material is a non-negligible factor affecting its sensitivity. The more negative charge the group has, the lower the sensitivity of the energetic material, otherwise the higher the sensitivity. It can be seen from Table 4 that with the increase of the positive electric field intensity, the charge of the nitro group gradually decreases, and the sensitivity of the cocrystal molecule decreases [36]. When a negative electric field is applied, as the

electric field intensity gradually increases, the charge of the nitro group gradually increases, indicating that the sensitivity of the cocrystal molecule increases.

Table.4 Nitro group charge of cocrystal molecules under different external electric fields.

	External electric field/a.u.	Q_{NO_2} /a.u.	ΔQ_{NO_2} /a.u.
CL-20/1,4-DNI	0.010	0.3050	-0.0904
	0.0075	0.3305	-0.0649
	0.005	0.3859	-0.0095
	0.000	0.3954	0.0000
	-0.005	0.4053	0.0099
	-0.0075	0.4115	0.0161
	-0.010	0.4328	0.0374
CL-20/2,4-MDNI	0.010	0.5051	-0.0418
	0.0075	0.5365	-0.0104
	0.005	0.5418	-0.0051
	0.000	0.5469	0.0000
	-0.005	0.5802	0.0333
	-0.0075	0.6103	0.0634
	-0.010	0.6427	0.0958
CL-20/4,5-MDNI	0.010	0.4081	-0.0391
	0.0075	0.4149	-0.0323
	0.005	0.4381	-0.0091
	0.000	0.4472	0.0000
	-0.005	0.4674	0.0202
	-0.0075	0.4714	0.0242
	-0.010	0.4772	0.0300

In order to explore the variation of the nitro group charge (ΔQ_{NO_2}) under the electric field, a linear fitting was performed on the change of the nitro group charge in the electric field. As shown in Fig.8, the linear correlation coefficients of the three cocrystals are 0.996 (CL-20/1,4-DNI), 0.989 (CL-20/2,4-MDNI)

and 0.965 (CL-20/4,5-MDNI), respectively. There is a good linear correlation between the charge change of the nitro group and the external electric field, indicating that the external electric field has a significant influence on the charge of the nitro group and the sensitivity of the energetic cocrystals [37].

4 Conclusion

In this work, DFT was used to systematically study the trigger bond, molecular orbital, electrostatic potential and nitro group charge of three CL-20/nitroimidazoles energetic cocrystal compounds in different electric field. The results are summarized as follows:

1 By analyzing the bond length changes and BDEs of the trigger bonds in the electric field, it can be concluded that as the positive electric field intensity increases, the trigger bonds become longer and the BDEs become smaller, resulting in an increase of the cocrystal sensitivity. The situation is reversed in the negative electric field.

2 Molecular orbital analysis shows that the positive electric field reduces the HOMO-LUMO energy gap of the cocrystals. CL-20/2,4-MDNI has the smallest energy gap among the three cocrystals, and its chemical reaction activity is higher than other cocrystals. Therefore, the mechanical sensitivity of CL-20/2,4-MDNI is the highest among the three cocrystals.

3 The ESP analysis shows that as the positive electric field intensity gradually increases, the $V_{s,max}$ of the three cocrystal molecules increases, so the sensitivity gradually increases. The situation is reversed in the negative electric field.

4 The charge analysis of the nitro group shows that as the positive electric field intensity increases, the charge of the nitro group decreases, resulting in a decrease in the sensitivity of the cocrystals. The situation is reversed in the negative electric field.

Declarations

Funding: This study was funded by the Natural Science Foundation of the Jiangsu Higher Education Institutions of China (20KJB620001) and National Natural Science Foundation of China (Grant No.11702129).

Conflicts of interest/Competing interests: No conflict of interest exists in the submission of this manuscript. The manuscript has not been published before nor submitted to another journal for the consideration of publication.

Availability of data and material: All data generated or analyzed during this study are included in this published article.

Code availability: Not applicable.

Authors' contributions: Conceptualization: Peng Ma, Xiaosong Xu; Methodology: Peng Ma; Formal analysis and investigation: Wenxin Xia, Renfa Zhang; Writing - original draft preparation: Xiaosong Xu; Writing - review and editing: Xiaosong Xu, Peng Ma; Funding acquisition: Peng Ma, Congming Ma; Resources: Yong Pan; Supervision: Juncheng Jiang.

Ethics approval: Not applicable.

Consent to participate: Not applicable.

Consent for publication: This manuscript is approved by all authors for publication.

Acknowledgments

We are grateful to the High-Performance Computing Center of Nanjing Tech University for supporting the computational resources.

References

1. Striebich RC, Lawrence J (2003) Thermal decomposition of high-energy density materials at high pressure and temperature. *J Anal Appl Pyrol* 70(2):339–352. [https://doi.org/10.1016/S0165-2370\(02\)00181-X](https://doi.org/10.1016/S0165-2370(02)00181-X)
2. Xu X, Xiao H, Ju X et al (2006) Computational studies on polynitrohexaazaadamantanes as potential high energy density materials. *The Journal of Physical Chemistry A* 110(17):5929–5933. <https://doi.org/10.1021/jp0575557>
3. Ma P, Wang J, Zhai D et al (2019) Structural transformation and absorption properties of 2,4,6-Trinitro-2,4,6-triazacyclohexanone under high pressures. *J Mol Struct* 1196:691–698. <https://doi.org/10.1016/j.molstruc.2019.07.020>
4. Hao L, Liu X, Zhai D et al (2020) Theoretical Studies on the Performance of HMX with different energetic groups. *ACS Omega* 5(46):29922–29934. <https://doi.org/10.1021/acsomega.0c04237>
5. Ren F, Cao D, Shi W et al (2017) A dynamic prediction of stability for nitromethane in external electric field. *RSC Adv* 7(74):47063–47072. <https://doi.org/10.1039/C7RA06290G>
6. Li Z, Huang H, Zhang T et al (2015) Electric-field-induced structural and electronic changes and decomposition of an energetic complex: a computational study on zinc carbonylhydrazide perchlorate crystals. *RSC Advances* 5(29):22601–22608. <https://doi.org/10.1039/C4RA15325A>
7. Ma P, Pan Y, Jiang J et al (2018) Molecular dynamic simulation and density functional theory insight into the nitrogen rich explosive 1,5-diaminotetrazole (DAT). *Procedia Eng* 211:546–554. <https://doi.org/10.1016/j.proeng.2017.12.047>
8. Duan B, Shu Y, Liu N et al (2018) Direct insight into the formation driving force, sensitivity and detonation performance of the observed CL-20-based energetic cocrystals. *CrystEngComm* 20(38):5790–5800. <https://doi.org/10.1039/C8CE01132J>

9. Bolton O, Matzger AJ (2011) Improved stability and smart-material functionality realized in an energetic cocrystal. *Angew Chem Int Ed* 50(38):8960–8963.
<https://doi.org/10.1002/anie.201104164>
10. Millar DIA, Maynard-Casely HE, Allan DR et al (2012) Crystal engineering of energetic materials: cocrystals of CL-20. *CrystEngComm* 14(10):3742. <https://doi.org/10.1039/C2CE05796D>
11. Zhang C, Yang Z, Zhou X et al (2014) Evident hydrogen bonded chains building CL-20-based cocrystals. *Cryst Growth Des* 14(8):3923–3928. <https://doi.org/10.1021/cg500796r>
12. Hao L, Wang J, Zhai D et al (2020) Theoretical study on CL-20-based cocrystal energetic compounds in an external electric field. *ACS Omega* 5(24):14767–14775.
<https://doi.org/10.1021/acsomega.0c01643>
13. Hang G, Yu W, Wang T et al (2019) Theoretical investigations into effects of adulteration crystal defect on properties of CL-20/TNT cocrystal explosive. *Comput Mater Sci* 156:77–83.
<https://doi.org/10.1016/j.commatsci.2018.09.027>
14. Guo R, Tao J, Duan X et al (2020) Study on phonon spectra and heat capacities of CL-20/MTNP cocrystal and co-formers by density functional theory method. *J Mol Model* 26(6).
<https://doi.org/10.1007/s00894-020-04415-3>
15. Grecu T, Adams H, Hunter CA et al (2014) Virtual screening identifies new cocrystals of nalidixic acid. *Cryst Growth Des* 14(4):1749–1755. <https://doi.org/10.1021/cg401889h>
16. Wu J, Zhang J, Li T et al (2015) A novel cocrystal explosive NTO/TZTN with good comprehensive properties. *RSC Advances* 5(36):28354–28359. <https://doi.org/10.1039/C5RA01124H>
17. An C, Li H, Ye B et al (2017) Nano-CL-20/HMX cocrystal explosive for significantly reduced mechanical sensitivity. *Journal of Nanomaterials* 2017:1–7. <https://doi.org/10.1155/2017/3791320>
18. Yang Z, Wang H, Ma Y et al (2018) Isomeric cocrystals of CL-20: a promising strategy for development of high-performance explosives. *Cryst Growth Des* 18(11):6399–6403.
<https://doi.org/10.1021/acs.cgd.8b01068>
19. Tan Y, Yang Z, Wang H et al (2019) High energy explosive with low sensitivity: a new energetic cocrystal based on CL-20 and 1,4-DNI. *Cryst Growth Des* 19(8):4476–4482.
<https://doi.org/10.1021/acs.cgd.9b00250>
20. Li Z, Huang H, Zhang T et al (2015) Electric-field-induced structural and electronic changes and decomposition of crystalline lead azide: a computational study. *J Phys Chem C* 119(16):8431–8437.
<https://doi.org/10.1021/jp507822z>
21. Ren F, Cao D, Shi W et al (2015) A theoretical prediction of the possible trigger linkage of CH_3NO_2 and NH_2NO_2 in an external electric field. *J Mol Model* 21(6). <https://doi.org/10.1007/s00894-015-2699-9>
22. Ren F, Shi W, Cao D et al (2020) External electric field reduces the explosive sensitivity: a theoretical investigation into the hydrogen transference kinetics of the $\text{NH}_2\text{NO}_2 \cdots \text{H}_2\text{O}$ complex. *J Mol Model* 26(12). <https://doi.org/10.1007/s00894-020-04607-x>

23. Sun K, Zhang S, Ren F et al (2021) Theoretical prediction of the trigger linkage, cage strain, and explosive sensitivity of CL-20 in the external electric fields. *J Mol Model* 27(3).
<https://doi.org/10.1007/s00894-020-04634-8>
24. Wu X, Liu Z, Zhu W (2021) External electric field induced conformational changes as a buffer to increase the stability of CL-20/HMX cocrystal and its pure components. *Materials Today Communications* 26:101696. <https://doi.org/10.1016/j.mtcomm.2020.101696>
25. Murray JS, Concha MC, Politzer P (2009) Links between surface electrostatic potentials of energetic molecules, impact sensitivities and $C-NO_2/N-NO_2$ bond dissociation energies. *Mol Phys* 107(1):89–97. <https://doi.org/10.1080/00268970902744375>
26. Frisch MJ, Trucks GW, Schlegel HB et al. Gaussian 16 Rev. C.01[CP/OL]
27. Ren F, Cao D, Shi W et al (2015) A theoretical prediction of the possible trigger linkage of CH_3NO_2 and NH_2NO_2 in an external electric field. *J Mol Model* 21(6). <https://doi.org/10.1007/s00894-015-2699-9>
28. Brill TB, James KJ (1993) Kinetics and mechanisms of thermal decomposition of nitroaromatic explosives. *Chemical reviews* 93(8):2667–2692. <https://doi.org/10.1021/cr00024a005>
29. He P, Zhang JG, Wang K et al (2015) Extensive theoretical studies on two new members of the FOX-7 family: 5-(dinitromethylene)-1,4-dinitramino-tetrazole and 1,1'-dinitro-4,4'-diamino-5,5'-bitetrazole as energetic compounds. *Phys Chem Chem Phys* 17(8):5840–5848.
<https://doi.org/10.1039/c4cp04883k>
30. Li Y, Evans JNS (1995) The Fukui Function: a key concept linking frontier molecular orbital theory and the hard-soft-acid-base principle. *J Am Chem Soc* 117(29):7756–7759.
<https://doi.org/10.1021/ja00134a021>
31. Xie Z, Hu S, Cao X (2016) Theoretical insight into the influence of molecular ratio on the binding energy and mechanical property of HMX/2-picoline-N-oxide cocrystal, cooperativity effect and surface electrostatic potential. *Molecular physics* 114(14):2164–2176.
<https://doi.org/10.1080/00268976.2016.1190038>
32. Lu T, Chen F (2012) Multiwfn: a multifunctional wavefunction analyzer. *J Comput Chem* 33(5):580–592. <https://doi.org/10.1002/jcc.22885>
33. Zhai D, Ma C, Ma P et al (2021) Theoretical insight into different energetic groups on the performance of energetic materials featuring RDX ring. *Fuel* 294:120497.
<https://doi.org/10.1016/j.fuel.2021.120497>
34. Politzer P, Murray JS (2014) Impact sensitivity and crystal lattice compressibility/free space. *J Mol Model* 20(5). <https://doi.org/10.1007/s00894-014-2223-7>
35. Zhang C (2006) Investigation on the correlation between the interaction energies of all substituted groups and the molecular stabilities of nitro compounds. *The Journal of Physical Chemistry A* 110(51):14029–14035. <https://doi.org/10.1021/jp063734s>
36. Ma P, Liu X, Hao L et al (2020) Pressure induced structural behavior of energetic cocrystal TNT/TNB: a density functional theory study. *J Mol Model* 26(6):121. <https://doi.org/10.1007/s00894-020->

37. Ma P, Pan Y, Jiang J et al (2018) Molecular dynamic simulation and density functional theory insight into the nitrogen rich explosive 1,5-diaminotetrazole (DAT). Procedia Eng 211:546–554. <https://doi.org/10.1016/j.proeng.2017.12.047>

Figures

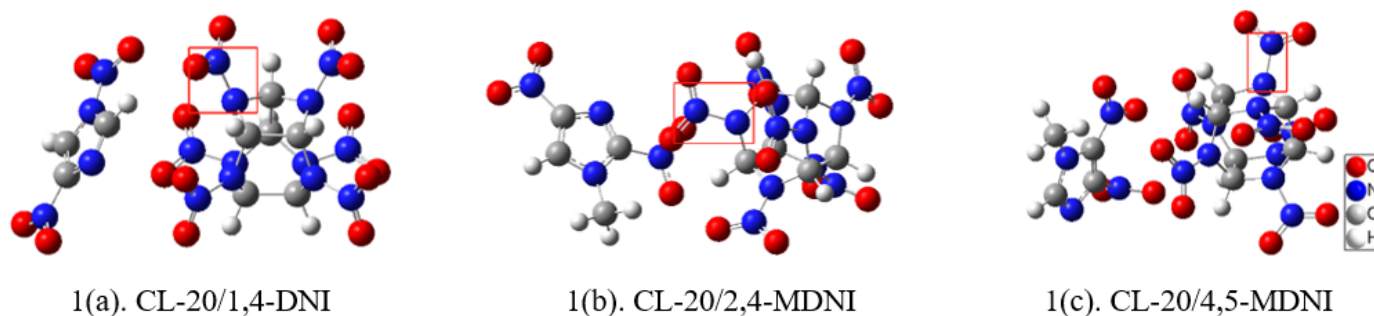


Figure 1

The optimized stable structure of CL-20/1,4-DNI, CL-20/2,4-MDNI and CL-20/4,5-MDNI

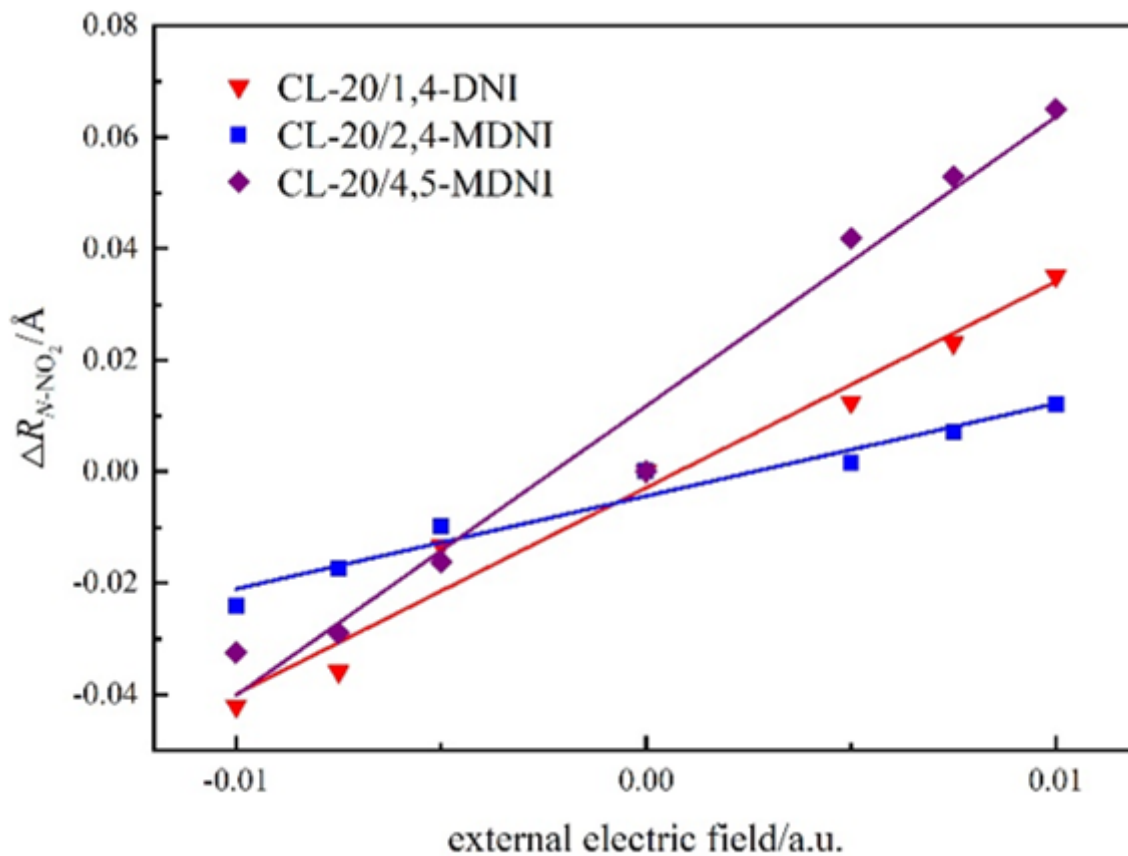
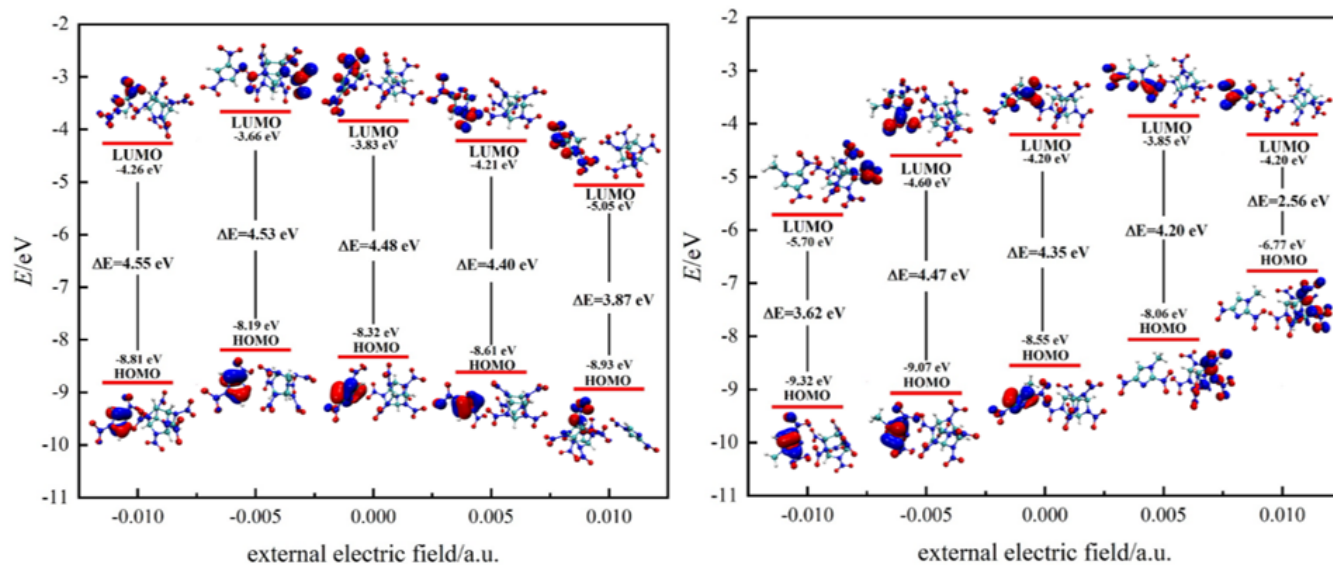


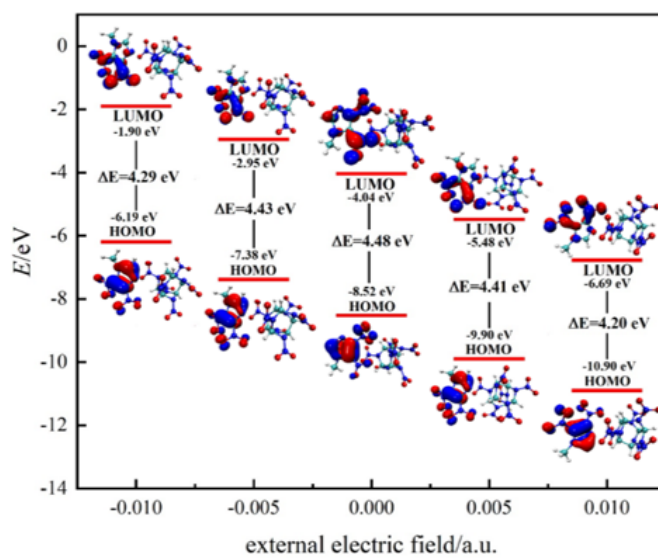
Figure 2

The linear fitting result of the trigger bond length of CL-20/1,4-DNI, CL-20/2,4-MDNI and CL-20/4,5-MDNI under the external electric field



3(a) CL-20/2,4-MDNI

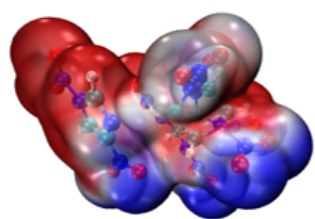
3(b) CL-20/2,4-MDNI



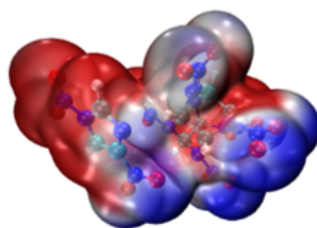
3(c) CL-20/4,5-MDNI

Figure 3

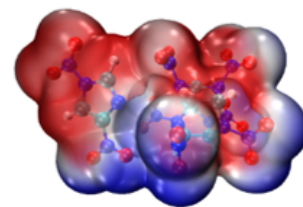
Orbital distribution and energy gap of CL-20/1,4-DNI, CL-20/2,4-MDNI and CL-20/4,5-MDNI



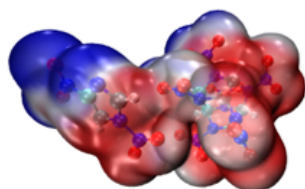
4(a). -0.01 a.u.



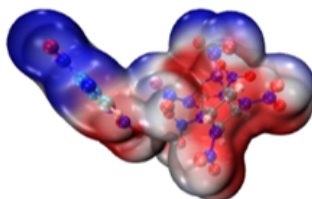
4(b). -0.0075 a.u.



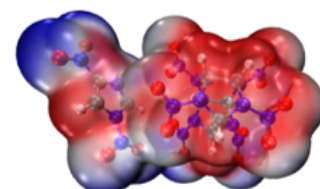
4(c). -0.005 a.u.



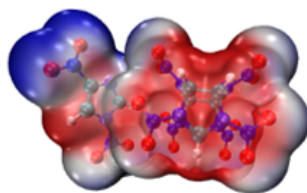
4(d). +0.01 a.u.



4(e). +0.0075 a.u.



4(f). +0.005 a.u.



4(g). 0.00 a.u.

Figure 4

Surface electrostatic potential for CL-20/1,4-DNI under different electric fields

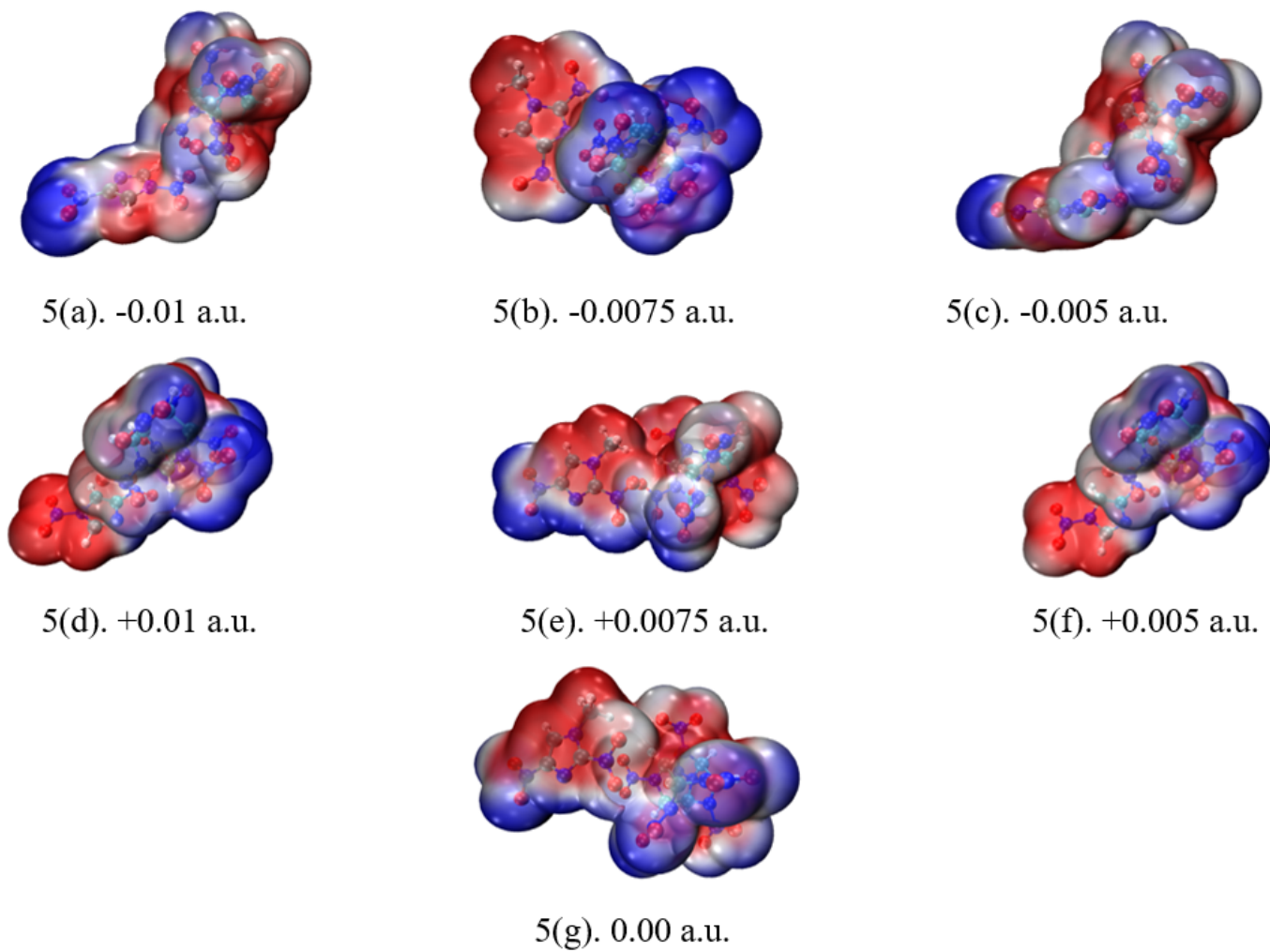
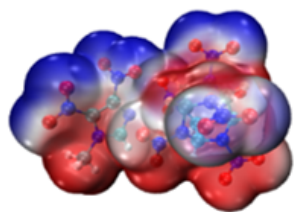
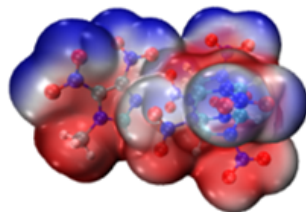


Figure 5

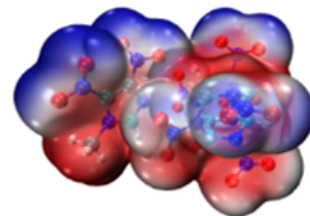
Surface electrostatic potential for CL-20/2,4-MDNI under different electric fields



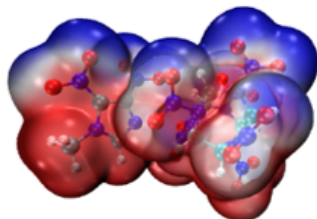
6(a). -0.01 a.u.



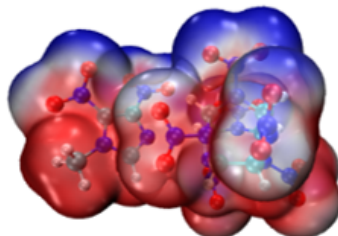
6(b). -0.0075 a.u.



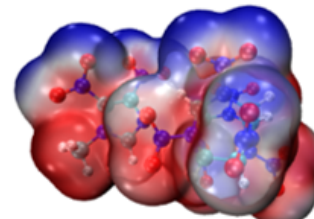
6(c). -0.005 a.u.



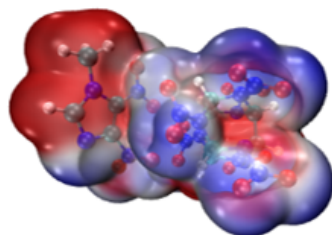
6(d). +0.01 a.u.



6(e). +0.0075 a.u.



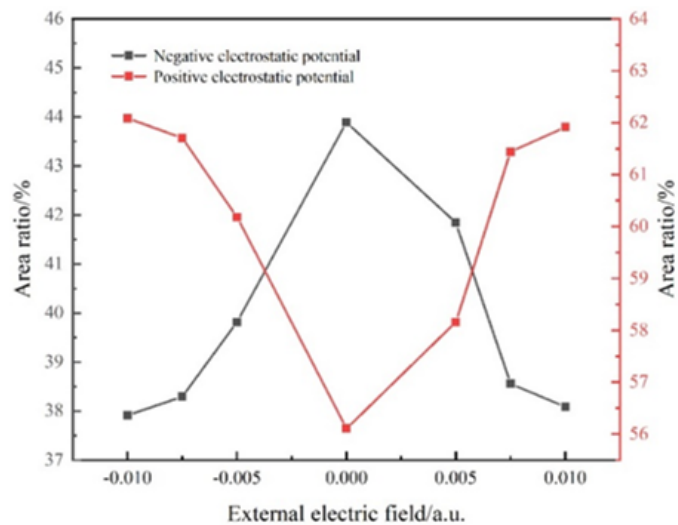
6(f). +0.005 a.u.



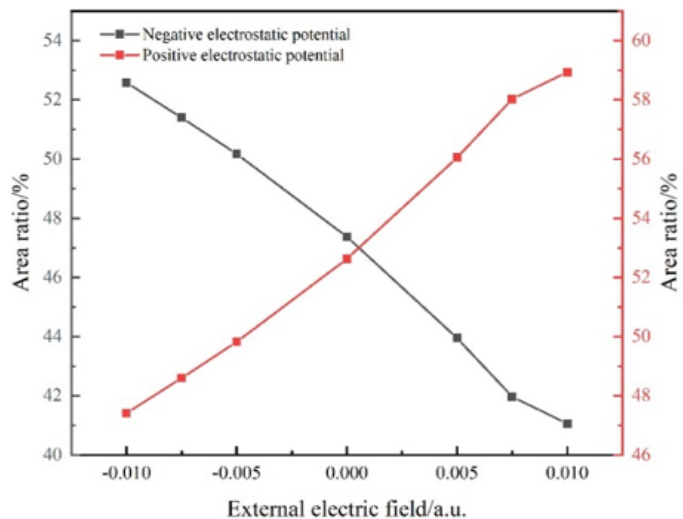
6(g). 0.00 a.u.

Figure 6

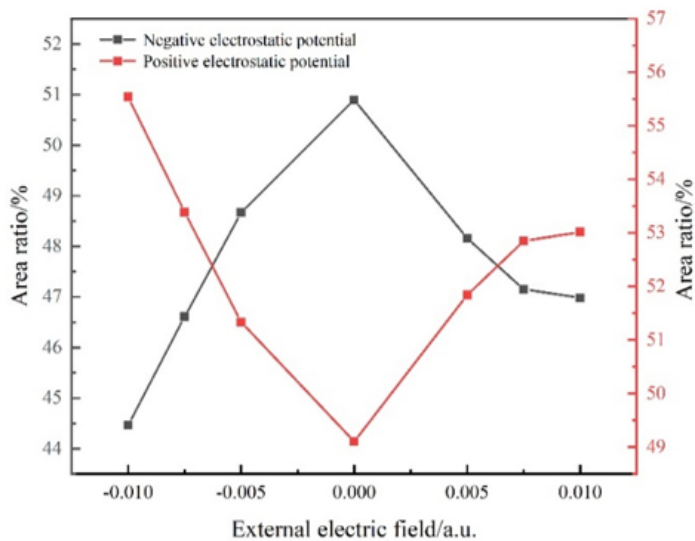
Surface electrostatic potential for CL-20/4,5-MDNI under different electric fields



7(a). CL-20/1,4-DNI



7(b). CL-20/2,4-MDNI



7(c). CL-20/4,5-MDNI

Figure 7

Proportion of positive and negative electrostatic potential area under different electric field strength

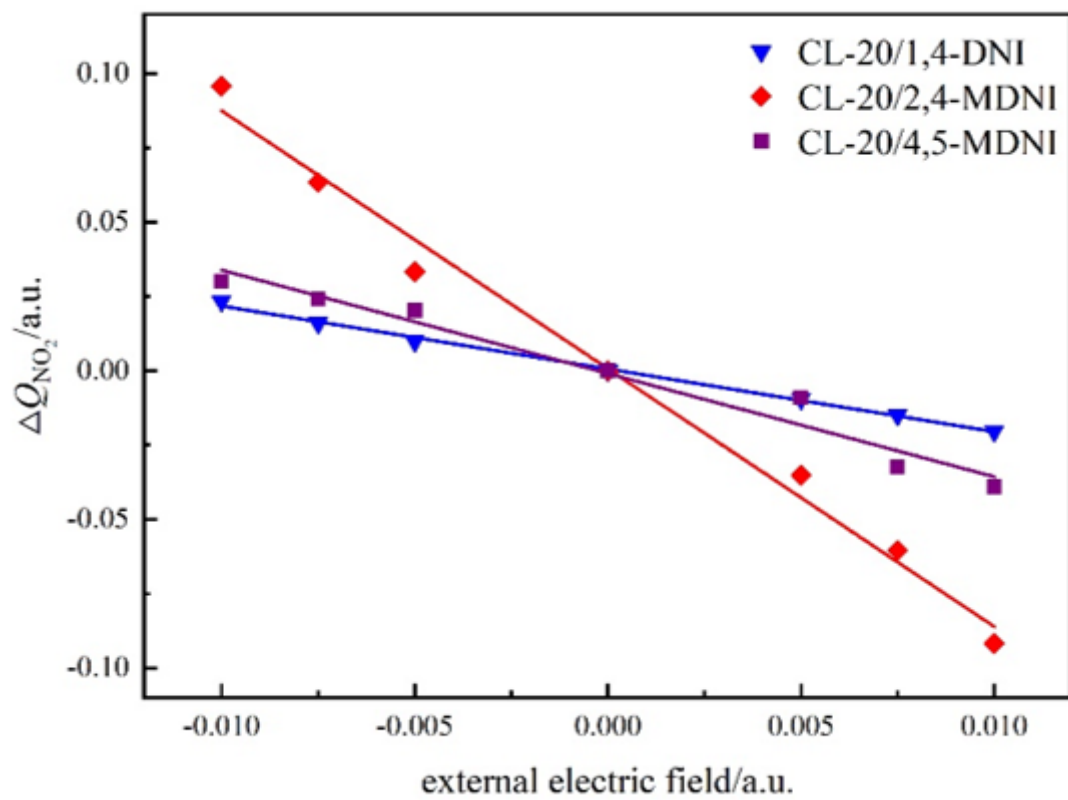


Figure 8

The linear fitting result of the nitro group charges of CL-20/1,4-DNI, CL-20/2,4-MDNI and CL-20/4,5-MDNI under the electric field